Available online at www.sciencedirect.com
SCIENCE DIRECT®
Journal of Nuclear Materials 355 (2006) 114–118
journal of nuclear materials
www.elsevier.com/locate/jnucmat

Thermal diffusivity of Americium mononitride from 373 to 1473 K

Tsuyoshi Nishi [a,*], Masahide Takano [a], Akinori Itoh [a], Mitsuo Akabori [a], Kazuo Minato [a], Minoru Kizaki [b]

[a] Nuclear Science and Engineering Directorate, Japan Atomic Energy Agency, Tokai-mura, Ibaraki-ken 319-1195, Japan
[b] Department of Hot Laboratories and Facilities, Japan Atomic Energy Agency, Tokai-mura, Ibaraki-ken 319-1195, Japan

Received 14 February 2006; accepted 27 April 2006

Abstract

The thermal diffusivity of AmN was measured from 373 to 1473 K by a laser flash method. The AmN sample was prepared from AmO_2 by the carbothermic reduction. The obtained AmN product was grinded and pressed at about 400 MPa to form a disk. The disk was sintered at 1823 K for 10 h in flowing $N_2 + 4\%H_2$ gas. The thermal diffusivity slightly decreased from 3.4×10^{-6} to 2.8×10^{-6} m^2/s with increasing temperature. As the specific heat capacity of AmN was not available in literature, the thermal conductivity of AmN was tentatively estimated from the measured thermal diffusivity, bulk density and the specific heat capacity of PuN. It was found that the thermal conductivity of AmN slightly increased with temperature. The thermal conductivity of AmN corrected to 100%TD was found to be smaller than those of UN, NpN and PuN, whereas that of AmN was larger than those of UO_2 and $(U_{0.8}Pu_{0.2})O_2$.

PACS: 65.40.−b; 81.05. Je

1. Introduction

The long-term hazard of radioactive wastes arising from nuclear energy production is a matter of discussion and public concern. In order to reduce the radiotoxicity of the high-level waste and to use the repository efficiently, burning or transmutation of minor actinides (MA: Np, Am, Cm) as well as plutonium is an option for the future nuclear fuel cycle. Many concepts have been proposed on the fuels together with advanced reactors or accelerator driven systems (ADS). Among various fuel types, nitrides are one of the candidates for the MA-bearing fuels because of high melting points, good thermal conductivities, and mutual solubility.

Thermal conductivities of MA nitrides are one of the most important thermophysical properties for the design of MA-bearing fuels and analysis of their behavior [1–4]. Several results have so far been reported for the thermal conductivities of uranium

* Corresponding author. Address: Research Group for Minor Actinides Properties, Division of Fuels and Materials Engineering, Nuclear Science and Engineering Directorate, Japan Atomic Energy Agency, Shirakata Shirane 2-4, Tokai-mura, Ibaraki-ken 319-1195, Japan. Tel.: +81 29 282 5431; fax: +81 29 282 5922.
E-mail address: nishi.tsuyoshi@jaea.go.jp (T. Nishi).

0022-3115/$ - see front matter © 2006 Elsevier B.V. All rights reserved.
doi:10.1016/j.jnucmat.2006.04.008

mononitride, UN [5], neptunium mononitride, NpN [6], and plutonium mononitride, PuN [5]. However, the thermal conductivity of Americium mononitride, AmN, is not available yet because the handling of AmN is not as easy as those of UN, NpN and PuN due to its radioisotopic and hydrolytic nature.

In this study, the thermal diffusivity of AmN was measured by the laser flash apparatus installed in a glove box with a highly-purified argon gas atmosphere. As the specific heat capacity of AmN was not available in literature, the thermal conductivity was tentatively estimated from the measured thermal diffusivity, bulk density and the specific heat capacity of PuN [7].

2. Experimental

2.1. Sample preparation

The AmN sample was prepared by the carbothermic reduction of Americium dioxide, AmO_2 [8]. The characteristics of starting material of AmO_2 are shown in Table 1. The AmO_2 powder was mixed with carbon powder at a molar C/Am ratio of 3.40. The mixture was compacted at 200 MPa and heated in a tungsten crucible at 1573 K in flowing N_2 gas at 500 ml/min. The CO gas release was measured continuously by an infrared spectrometer to monitor the conversion of the oxide to the nitride. The formation of the nitride was formally expressed by

$$AmO_2 + 2C + 1/2N_2 \rightarrow AmN + 2CO.$$

After the CO gas release subsided, the flowing gas was changed to $N_2 + 4\%H_2$ mixed gas to remove the residual carbon. This additional heating was done at 1773 K for 4.5 h and then at 1793 K for 5 h until the CO gas release subsided again.

The obtained AmN product was grinded and pressed at about 400 MPa to form a disk. The disk was sintered at 1823 K for 10 h in flowing $N_2 + 4\%H_2$ gas. The characteristics of sintered AmN sample are summarized in Table 2. The bulk density was calculated from the diameter, thickness and weight to be 10.56 Mg/m^3. The diameter and thickness were measured by a dial gauge to be 3.039 and 0.644 mm, respectively. The weight was measured by an electronic balance to be 49.34 mg. It was observed that the weight of the sample slightly decreased after the thermal diffusivity measurements. It was considered that the weight loss was probably due to evaporation of the sample during the measurements.

Table 1
Characteristics of AmO_2

Non-radioactive impurities mass fraction (Na, Ca, Si, Al, Fe, Mg, Cr, Ni, B, Ti)	<0.3%
Mass share of ^{243}Am in Am isotopic mixture	99.86%
Element mass fraction of ^{244}Cm	0.019%

Table 2
Characteristics of sintered AmN sample

	Before measurement	After measurement
Diameter (mm)	3.039 ± 0.006	3.040 ± 0.006
Thickness (mm)	0.644 ± 0.006	0.637 ± 0.006
Weight (mg)	49.34 ± 0.03	49.18 ± 0.03
Density (Mg/m^3)	10.56 ± 0.10	10.64 ± 0.10
Nitrogen (wt%)	–	5.13 ± 0.07
Oxygen (wt%)	–	0.55 ± 0.03
Carbon (wt%)	–	0.08 ± 0.02

After the thermal diffusivity measurements, the contents of oxygen, nitrogen and carbon were measured to determine the chemical composition of the AmN sample. The oxygen and nitrogen contents were measured with an apparatus (HORIBA, EMGA-550) based on the inert gas fusion technique. The carbon content was measured with an apparatus (CE Instruments, NC-2500) based on the combustion technique. The impurities of carbon and oxygen contained in the AmN sample were found to be less than 0.08 and 0.55 wt%, respectively. The AmN sample was examined by powder X-ray diffraction analysis with Cu-Kα radiation to determine the lattice parameter and to identify the phases. The AmN sample was grounded in an agate mortar in a glove box with purified argon gas atmosphere. The silicon powder was selected as a standard sample for X-ray diffraction analysis. Each of AmN and silicon powders was mounted on a holder with epoxy resin, and the surface was sealed with a polyimide film of 50 μm thickness to minimize the hydrolysis during the measurement. The AmN sample was scanned from 20 to 120° in 2θ at a step of 0.02°.

2.2. Thermal diffusivity measurement

The thermal diffusivity of the sintered AmN sample was measured by the laser flash method. The schematic diagram of the laser flash apparatus installed in the glove box with a highly-purified argon gas atmosphere is shown in Fig. 1. In the glove box, the oxygen and moisture contents were

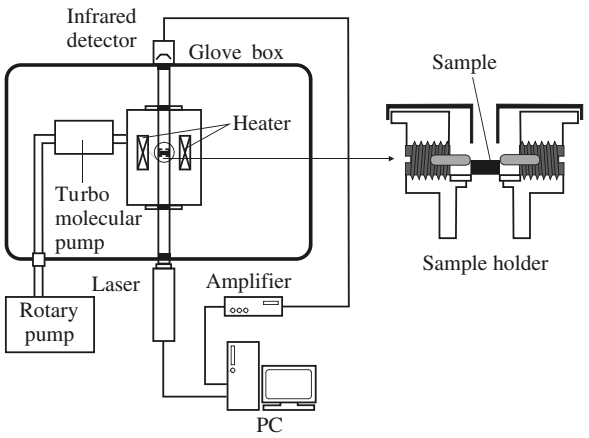

Fig. 1. Schematic diagram of the thermal diffusivity measurement apparatus for AmN.

controlled less than two and three ppm, respectively. Thus, it is possible to handle the AmN sample which is unstable in the air. The AmN sample was set in the sample holder applied to the vertical type laser flash apparatus and heated to the desired temperature with a Mo heater [9]. The thermal diffusivity measurements were performed from 373 to 1473 K in vacuum with background pressure of less than 2.5×10^{-4} Pa.

The thermal diffusivity was determined from the temperature rise at the rear surface of the sample measured with an InSb infrared detector after the front surface of the sample was instantaneously irradiated by a pulse of Nd glass laser. The data of temperature response curve at the rear surface was analyzed by the curve fitting method [10,11].

The half-time method [12] is often used to evaluate the thermal diffusivity. However, the thermal diffusivity evaluated by the half-time method is known to be more or less affected by radiative heat loss from the sample surface. The curve fitting method was, therefore, employed in this study to calculate the thermal diffusivity of the sintered AmN sample. In the curve fitting method, the thermal diffusivity is obtained by fitting the following equation to the measured temperature rise, ΔT, with a least square method.

$$\Delta T = \Delta T_{\mathrm{m}} \sum_{n=0}^{\infty} A_n \exp\left[-\left(\frac{X_n}{\pi}\right)^2 \frac{t}{t_0}\right], \qquad (1)$$

where ΔT_{m} is the maximum temperature rise, A_n and X_n are the functions of radiative heat loss, t is the time after the irradiation of the sample, $t_0 = l^2/(\pi^2\alpha)$, l is the thickness of the sample and α is the thermal diffusivity of the sample. It is also worth noting that the maximum temperature rise and radiative heat loss are obtained together with the thermal diffusivity.

In order to examine the total measuring accuracy of the experimental system, the thermal diffusivities of tantalum, nickel and the sintered cerium oxide were measured from 298 to 1573 K. The sizes of tantalum, nickel and the sintered cerium oxide were from 3 to 5 mm in diameter and from 1 to 2 mm in thickness. It was elucidated that the uncertainty of the thermal diffusivity values obtained with this system was estimated to be less than 5% in comparison with literature values [9].

3. Results and discussion

The thermal diffusivity measurements were performed in both heating and cooling processes for three times. The first measurement was performed from 373 to 1273 K in heating process (Run 1). The second measurement was performed from 1273 to 1473 K in heating process and then from 1473 to 523 K in cooling process (Run 2). The final measurement was performed from 373 to 523 K in heating process (Run 3). The measured thermal diffusivities are shown in Fig. 2. It was found that good reproducibility of the experimental thermal diffusivity data was confirmed by the heating and cooling measurements. The deviation of thermal diffusivities obtained in both heating and cooling processes was within 5%. As shown in Fig. 2, the thermal diffusivity of AmN slightly decreased from 3.4×10^{-6} to 2.8×10^{-6} m^2/s with increasing temperature from 373 to 1473 K.

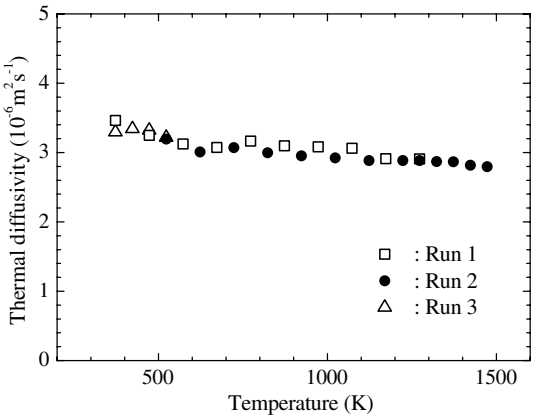

Fig. 2. Thermal diffusivity of sintered AmN sample (77.5%TD).

After the thermal diffusivity measurements, the AmN sample was examined by powder X-ray diffraction analysis to determine the lattice parameter and to identify the phases. The lattice parameter was determined to be 0.5003 ± 0.0001 nm. Since the theoretical density of AmN was calculated from the atomic weight and lattice parameter to be 13.62 Mg/m^3, the relative density of the AmN sample for the thermal diffusivity measurements corresponded to 77.5%TD (TD: theoretical density). The X-ray diffraction pattern suggested that oxide phases in the AmN sample were scarcely observed. Thus, it was considered that no significant oxidation of the AmN sample occurred during the measurements.

Furthermore, the thermal conductivities of AmN with 77.5%TD and corrected to 100%TD were estimated. The thermal conductivity, λ, can be estimated by the following equation:

$$\lambda = \alpha C_p \rho, \tag{2}$$

where C_p is the specific heat capacity and ρ is the bulk density of the sample. The specific heat capacity of AmN was not available unfortunately. The specific heat capacities of PuN [7] are nearly equal to those of UN [13] and NpN [14]. In addition, the element of Pu is next to that of Am in periodic table. Thus, the specific heat capacity of AmN was substituted by that of PuN.

In order to estimate the thermal conductivity with 100%TD, the present data were corrected by the analytical equation of Schulz [15]

$$\lambda = \lambda_{TD}(1 - P)^X, \tag{3}$$

where λ_{TD} is the thermal conductivity of the sample with 100%TD, P is the porosity of the sample and $X = 1.5$ is the parameter for closed pores of spherical shape. Among a variety of porosity correction formulas, Eq. (3) was in best agreement with the result of the finite element computations in the wide range of the porosity up to 0.3 as reported by Bakker et al. [16].

The thermal conductivities of AmN with 77.5%TD and corrected to 100%TD are shown in Fig. 3, together with those of UN [5], NpN [6] and PuN [5]. It was found that the thermal conductivity of AmN gradually increased with temperature over the temperature range investigated, which was the same tendency as UN, NpN and PuN. According to the literature [17,18], the thermal conductivities of UN and PuN slightly increased with

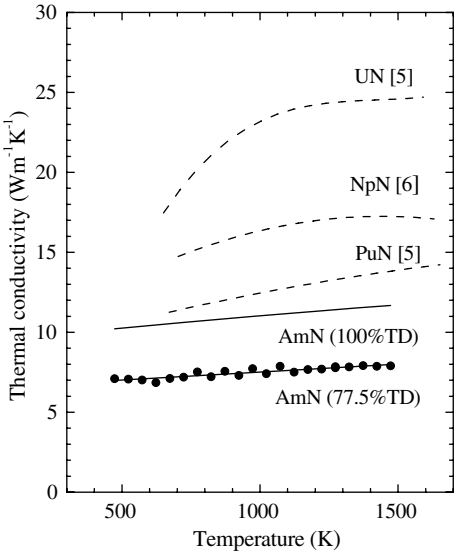

Fig. 3. Thermal conductivities of AmN with 77.5%TD and corrected values to 100%TD (solid lines), together with those for UN [5], NpN [6], PuN [5] (broken lines).

temperature due to the electrical component. It can be presumed that the increase in the thermal conductivity of AmN is probably due to the electrical component. It was also found that the thermal conductivities of actinide nitrides were decreased with increasing atomic number from U to Am. Actually, the electrical conductivities of UN, NpN

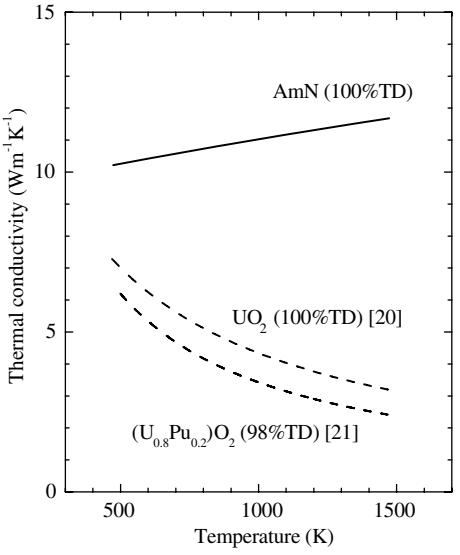

Fig. 4. Estimated thermal conductivity of AmN with 100%TD (solid line), together with those for UO_2 [20] and $(U_{0.8}Pu_{0.2})O_2$ [21] (broken lines).

and PuN have a tendency to decrease with increasing atomic number from U to Pu [19]. Thus, it was consistent that the thermal conductivity of AmN was smaller than those of UN, NpN and PuN.

The thermal conductivity of AmN, corrected to 100%TD, is shown in Fig. 4 together with those of UO_2 [20] and $(U_{0.8}Pu_{0.2})O_2$ [21]. It was found that the thermal conductivity of AmN was still larger than those of UO_2 and $(U_{0.8}Pu_{0.2})O_2$ in the temperature range from 473 to 1473 K. The results agree with the fact that the main thermal transport mechanism of UO_2 and $(U_{0.8}Pu_{0.2})O_2$ is likely explained by phonon, whereas that of actinide nitrides is quite likely to be controlled by the electron transport.

4. Conclusions

The AmN sample was prepared by the carbothermic reduction of AmO_2. The thermal diffusivity of AmN was successfully measured by the laser flash method in the temperature range from 373 to 1473 K. The conclusions were as follows:

(1) The thermal diffusivity of AmN slightly decreased from 3.4×10^{-6} to 2.8×10^{-6} m^2/s with increasing temperature from 373 to 1473 K.
(2) The thermal conductivity of AmN was estimated from the measured thermal diffusivity, bulk density and the specific heat capacity of PuN. That of AmN corrected to 100%TD gradually increased with temperature over the temperature range investigated, which was the same tendency as UN, NpN and PuN. It can be presumed that the increase in the thermal conductivity of AmN is probably due to the electrical component.
(3) The thermal conductivity of AmN corrected to 100%TD was smaller than those of UN, NpN and PuN, whereas that of AmN was larger than those of UO_2 and $(U_{0.8}Pu_{0.2})O_2$. The results agree with the fact that the main thermal transport mechanism of UO_2 and $(U_{0.8}Pu_{0.2})O_2$ is likely explained by phonon, whereas that of actinide nitrides is quite likely to be controlled by the electron transport.

Acknowledgements

The study was carried out within the task 'Technological development of a nuclear fuel cycle based on nitride fuel and pyrochemical reprocessing' entrusted from the Ministry of Education, Culture, Sports, Science and Technology of Japan. The authors are grateful to M. Numata and T. Tomita, Department of Hot Laboratories and Facilities, JAEA and M. Kamoshida, Chiyoda Maintenance Corporation for their kind supports.

References

[1] M. Mignanelli, R. Thetford, OECD/NEA (2001) 161.
[2] K. Minato, Y. Arai, M. Akabori, K. Nakajima, Research on nitride fuel for transmutation of minor actinides, in: Proc. AccApp/ADTTA '01, Reno, Nevada, November 11–15, 2001 CD-ROM, 2001.
[3] K. Minato, M. Akabori, M. Takano, Y. Arai, K. Nakajima, A. Itoh, T. Ogawa, J. Nucl. Mater. 320 (2003) 18.
[4] R. Thetford, M. Mignanelli, J. Nucl. Mater. 320 (2003) 44.
[5] Y. Arai, Y. Suzuki, T. Iwai, T. Ohmichi, J. Nucl. Mater. 195 (1992) 37.
[6] Y. Arai, Y. Okamoto, Y. Suzuki, J. Nucl. Mater. 211 (1994) 248.
[7] F.L. Oetting, J. Chem. Thermodynam. 10 (1978) 941.
[8] M. Takano, A. Itoh, M. Akabori, T. Ogawa, S. Kikkawa, H. Okamoto, Synthesis of Americium mononitride by carbothermic reduction method, in: Proc. Global'99, Jackson Hole, USA, August 29–September 3, 1999 CD-ROM, 1999.
[9] T. Nishi, M. Takano, A. Itoh, M. Akabori, K. Minato, M. Kizaki, JAERI-Tech 2005-051 (2005), in Japanese.
[10] A. Cezairliyan, T. Baba, R. Taylor, Int. J. Thermophys. 15 (1994) 317.
[11] D. Josell, J. Warren, A. Cezairliyan, J. Appl. Phys. 78 (1995) 6867.
[12] W.J. Parker, R.J. Jenkins, C.P. Butler, G.L. Abbott, J. Appl. Phys. 32 (1961) 1679.
[13] F.L. Oetting, J.M. Leitnaker, J. Chem. Thermodynam. 4 (1972) 199.
[14] K. Nakajima, Y. Arai, J. Nucl. Sci. Technol. 3 (Supplement) (2002) 620.
[15] B. Schulz, High Temp.-High Press. 13 (1981) 649.
[16] K. Bakker, H. Kwast, E.H.P. Cordfunke, J. Nucl. Mater. 223 (1995) 135.
[17] R.W. Endebrook, E.L. Foster, D.L. Keller, US Report BMI-1690, 1964.
[18] D.L. Keller, US Report BMI-1809, 1967.
[19] Y. Arai, K. Nakajima, Y. Suzuki, J. Alloys. Comp. 271–273 (1998) 602.
[20] P.G. Lucuta, Hj. Matzke, R.A. Verrall, J. Nucl. Mater. 223 (1995) 51.
[21] R.L. Gibby, J. Nucl. Mater. 38 (1971) 163.